



Optimization of printing parameters in fused deposition modeling for improving part quality and process sustainability

Carmita Camposeco-Negrete¹

Received: 10 March 2020 / Accepted: 25 May 2020 / Published online: 5 June 2020
© Springer-Verlag London Ltd., part of Springer Nature 2020

Abstract

Additive manufacturing (AM) technology is capable of efficiently building complex shapes when compared with traditional manufacturing methods. Fused deposition modeling (FDM) is one of the AM processes, and it produces a great variety of polymeric parts. Therefore, it is essential to determine the relationship that exists among its process parameters, productivity and sustainability, quality of the final piece, and its structural performance. This paper presents an experimental study centered on optimizing five responses associated with FDM: energy consumption of the 3D printer, processing time, part's dimensional accuracy, the quantity of material used to print the pieces, and mechanical strength of the specimens. The model material employed was acrylonitrile styrene acrylate. The effects of five key process parameters on the responses were studied using the Taguchi methodology and analysis of variance (ANOVA). These parameters were layer thickness, filling pattern, orientation angle, printing plane, and position of the piece on the build platform. A desirability analysis was employed to determine the set of process parameters that provided the best trade-off among all the considered variables. The results showed that the approach presented in this work allowed for simultaneous optimization of all the observed variables for the 3D printing process.

Keywords Material extrusion · 3D printing · Optimization · Sustainability · Mechanical properties

1 Introduction

Over the past years, additive manufacturing (AM) processes have evolved from just being employed in rapid prototyping techniques to assist in manufacturing methods [3]. The latter aims to produce finished parts that are economically feasible, robust, with high strength, and with long-term stability. Moreover, these processes do not require special or costly tooling for manufacturing the parts, which allows the AM machine to handle a variety of polymers [7].

Material extrusion [1] is an additive manufacturing process preferred for building components due to its low cost, ease of creating complex shapes, and reduced waste. This process is also known as fused filament fabrication (FFF) or fused deposition modeling (FDM), which is a trademark name. The FDM

method starts by selectively dispensing material through a nozzle. The polymer is then melted and forced out of the outlet by applying pressure. The polymer, when extruded, is in a semisolid state, and it solidifies and bonds with the already extruded material [16]. The nozzle is capable of moving in the XY plane, while the build platform moves along the z axis. In this way, FDM technology allows for complex shapes and internal structures [7].

For many polymers, building material and support material are used during the FDM process. Both of them are heated and extruded using different nozzles. The support material holds the structure while printing the layers of the piece. Since this material does not adhere to the build polymer, it can be removed by submerging the part in a bath [13].

Despite being a technology that provides several benefits, material extrusion is a manufacturing process that requires some attention regarding its energy consumption. Because such electricity is obtained from fossil fuel sources, it generates an environmental impact. As a consequence, it is vital to optimizing the energy consumption of the FDM process, along with the typical operation measures (productivity, quality, and structural performance of the part).

✉ Carmita Camposeco-Negrete
carmitacamposeco@tec.mx

¹ School of Engineering and Science, Tecnológico de Monterrey, Eduardo Monroy Cárdenas 2000, 50110 Toluca, Estado de México, Mexico

2 Literature review

In the past several years, researchers have examined the outcomes of 3D printing parameters on key metrics of FDM to improve the condition of the part, decrease the building cycle, and guarantee reliable structural performance by maximizing yield strength and ultimate tensile strength, among other mechanical properties.

Hassanifard and Hashemi [10] studied the effect of part's build orientation and raster angle on the strain-life fatigue of specimens made of Ultem 9085, polycarbonate (PC), and polylactic acid (PLA). Parts were created based on ASTM D638-14 and ASTM D790-17 standards. The authors concluded that infill density affected the mechanical properties of the printed part.

The aim of the work reported by Verbeeten et al. [24] was to investigate the strain-rate dependence of the yield stress for tensile samples made of PLA, based on ISO 527-2 standard. Printing speed, infill orientation angle, and bed temperature were modified. One of the conclusions of the study was that a change of infill orientation angle from 0 to 90° provided anisotropic effects to the pieces.

Zhao et al. [26] explored the effect of printing angle and layer thickness on the mechanical properties of specimens made of PLA. The standard used to fabricate the units was ISO 527-2-2012. Tensile strength increased with higher values of printing angle and reduced ones of layer thickness.

Tanoto et al. [23] evaluated dimensional accuracy, processing time, and tensile strength of 3D printed components. The components were made of ABS, using FDM technology. The printing plane and the orientation angle were selected as the response variables to be analyzed. The specimens employed in the experimental trials belong to type IV, according to the ASTM D638-02 standard. Printing time diminished when the part was oriented in the XZ plane at 90°. This orientation also provided a specimen's length value closer to the one of the ASTM standard.

The work of Alafaghani et al. [2] presented an experiment to determine the values of infill rate, infill pattern, the orientation of the part, and layer thickness that enhanced dimensional accuracy and mechanical properties of specimens made of PLA. The part design followed type IV specifications according to the ASTM D638-15 standard. Lower values of fill density and shell thickness and higher values of layer thickness and feed rate reduced the measured values.

Huynh et al. [11] considered the effect of infill rate, infill pattern, and layer thickness on the dimensional precision of parts made of PLA using FDM. The piece was a CAD model created by the authors, and an orthogonal array L27 was applied, along with a fuzzy approach to optimize printing parameters.

The work of Padhi et al. [14] shows a comparison between the dimensional deviation of printed specimens from the

dimensions of a CAD model. An L27 orthogonal array allowed to modify the infill angle, raster width, air gap, orientation of the part, and layer thickness. The material of the specimens is ABS P400. A medium value for layer thickness and raster width, the greatest one for the air gap and the least for orientation and raster angle, granted the highest dimensional precision.

Mohamed et al. [12] investigated the dimensional accuracy of specimens made of a PC-ABS blend, employing FDM. The process parameters that were modified are raster angle, raster width, air gap, part orientation, layer thickness, and the number of contours. The geometry of the specimens is according to the standards ASTM D5418-07 and ASTM D7028-07e1. The layer thickness was the factor that affected all the responses.

Raut et al. [17] analyzed the tensile and flexural behavior, as well as the processing time of specimens made of ABS P400, following the standards ASTM D638 and ASTM D790. The process parameter that was varied was the orientation of the piece on the build platform. This parameter has a significant effect on all the studied variables.

Peng et al. [15] investigated the relationship among dimensional accuracy, processing time, and layer thickness during 3D printing of specimens made of ABS. The authors developed the geometry employed in the experiment, and they used the response surface method (RSM) along with a fuzzy interference system to improve process metrics. Warp deformation diminished with an increase of layer thickness, and a reduction of filling velocity.

Material extrusion has gained the attention of various researchers that aim to improve the characteristics and functionality of parts produced by this method, using different optimization techniques. Nevertheless, there are little efforts toward the optimization of process parameters for components made of ASA.

ASA is the acronym for acrylonitrile styrene acrylate. It is a thermoplastic used in the automotive industry due to its good toughness, rigidity, durability, and resistance to weather conditions, mainly water and UV radiation. This polymer has higher endurance compared with ABS, which is the most widespread material applied for FDM [9]. Consequently, it is essential to study the performance of this thermoplastic when printed using FDM.

Manufacturing a product is only one step of its life cycle, and each stage of the period has associated environmental, health, and safety consequences. However, the information concerning energy consumption is not available for all the manufacturing processes. As a consequence, researchers have started to generate this information. A competitive organization should know the energy consumed by all manufacturing operations to avoid or minimize all costs concerned with being or not being environmentally friendly [21].

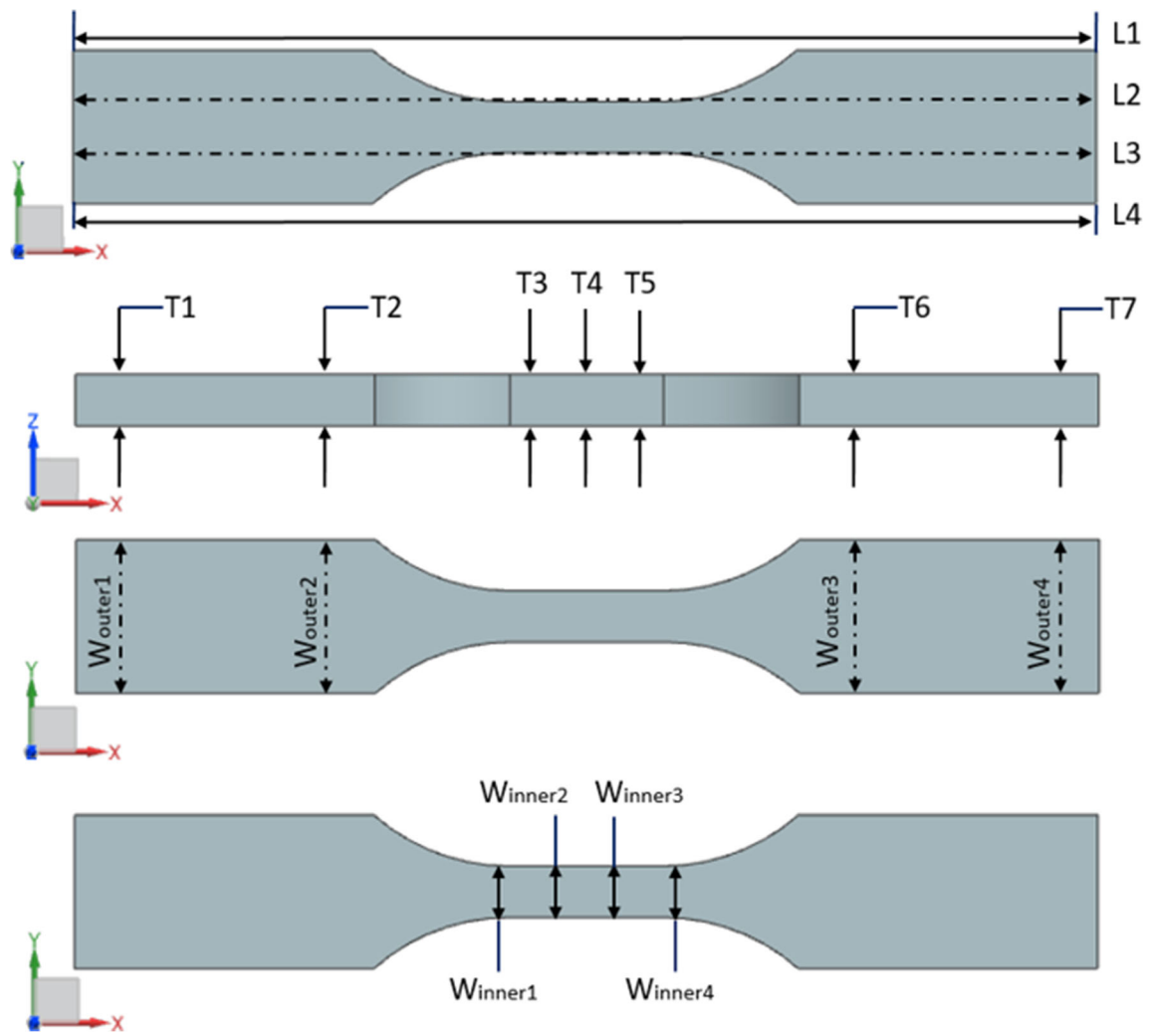


Fig. 1 Measurement locations of the printed part



Fig. 2 From left to right: MTS 810 material testing system, specimen before the test, specimen after the test

Although a vast number of researchers have made efforts in the field of FDM, it is necessary to obtain the best process parameters related to this manufacturing operation. Energy consumption and time effectiveness are features associated with sustainable manufacturing. The former has an influential connection with carbon emissions, and the latter is connected to sustainability; the longer the time, the greater the energy spent by the 3D printer, as well as the human means applied during its service. The quantity of material demanded to build the part influences the sustainability of the process due to the carbon emissions released during its fabrication. Moreover, all these factors are related to the product's total cost [4].

The present document outlines an experimental study to optimize five primary responses of the FDM process: processing time, energy spent by the 3D printer, dimensional precision of the pieces, the quantity of polymer used for printing the parts, and mechanical attributes of the specimens. Five process parameters were modified to study their influence on the variables. These parameters were layer thickness, filling pattern, the orientation angle of the piece, printing plane, and position of the specimen on the build platform.

The Taguchi methodology was employed to analyze the effects of the process parameters on the response variables. An L27 orthogonal array comprised the experimental trials, and an analysis of variance (ANOVA), signal to noise (S/N) ratio, and means graphs helped to determine the optimum values for each of the parameters. A desirability analysis was selected to define a set of parameters that optimized all the variables at the same time. The results showed that it was possible to obtain a trade-off among all the fundamental metrics while enhancing process sustainability and part quality.

3 Experimental procedure for the ME process

3.1 Part to be manufactured, materials, and 3D printer specifications

The geometry and dimensions of the printed part are the ones specified for type V specimen, according to the ASTM D638-14 standard. The NX 11.0 software from Siemens was employed to model the part. The building material was ASA Ivory, and the soluble support material was QSR. Both of them were of natural color, manufactured by Stratasys.

An F270 printer from Stratasys built the parts. This printer has a calibration routine used before printing any

Fig. 3 Filling patterns selected

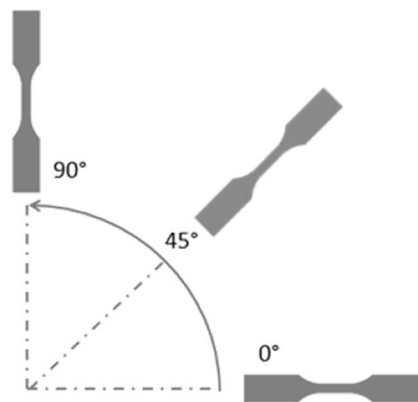
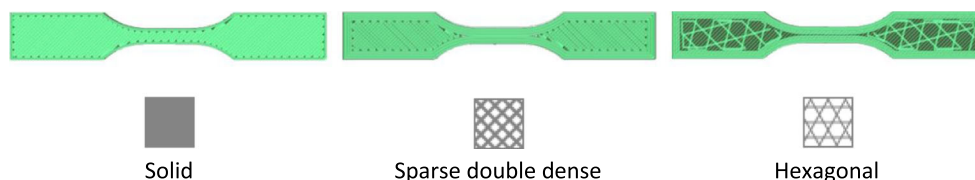


Fig. 4 Orientation angles of the specimen on the printing plane

of the specimens. The GrabCAD software aided to process the files of the pieces and send them to the F270 printer. This software can work with NX 11.0 native files (.prt extension) to set process parameters and estimate the quantity of material needed to print the part, as well as the processing time.

3.2 Processing time, energy consumption, dimensional accuracy, and mechanical property measurement system

The time needed to print the part was quantified using a stopwatch once the extrusion nozzle was moved to execute its first movement until it finished the piece. The energy drawn from the grid was collected using a power quality analyzer, named Fluke 43B. This equipment allowed to measure the average machine's power consumption while printing. Then, total energy consumed (in kWh) was determined by multiplying the value given by the Fluke 43B times the building time (in hours).

A Mitutoyo outside micrometer with an accuracy of 0.01 mm was employed to estimate the length (L), width (Wouter and Winner), and thickness (T) of the specimens (Fig. 1). Four measurements were obtained for each one of the dimensions (seven in the case of the thickness, as shown in Fig. 1), and they were averaged.

Dimensional accuracy was calculated using Eq. 1.

$$\Delta D = |D_{\text{EXP}} - D_{\text{DWG}}| \quad (1)$$

where ΔD is the deviation between the dimension established by the 3D model or drawing (D_{DWG}) according to ASTM D638-14 standard and the one obtained by

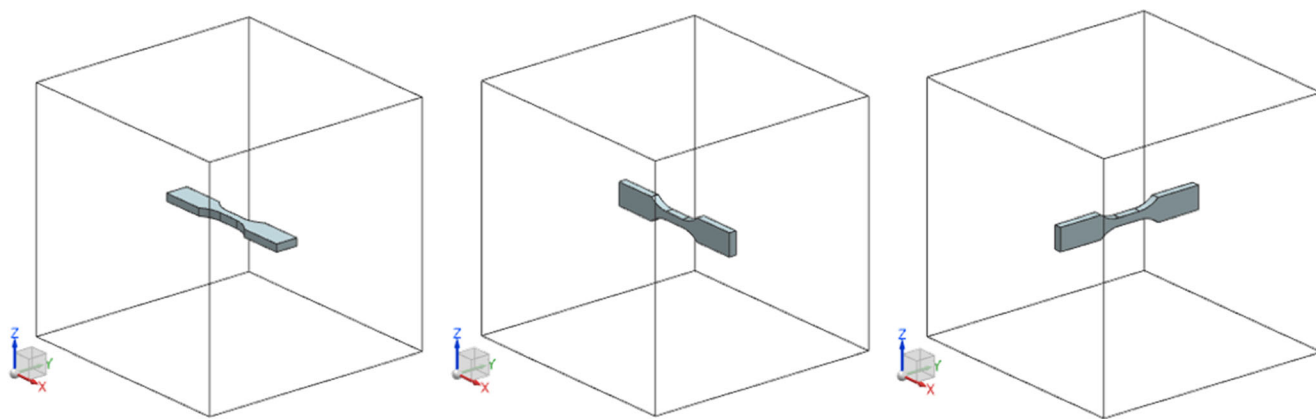


Fig. 5 Printing planes used for printing the specimens. The orientation angle of the specimen was set at 0° for the three planes shown

measuring the printed specimen (D_{EXP}). Dimensional accuracy is improved when the value of ΔD is close to zero.

Tensile tests were executed according to ASTM D638-14 standard, at a speed of testing of 1 mm/min. The tensile machine employed was an MTS 810 material testing system. Figure 2 exhibits the device and the specimen before and after one of the trials. Data obtained from the tests were analyzed using the Excel software to find out the values of yield strength (0.2% offset) and ultimate tensile strength for each specimen.

Lastly, the model and support material amounts needed to print each part were quantified using the estimation option included in the GrabCAD software.

3.3 Input process parameters of the ME

3.3.1 Layer thickness

This parameter is associated with the height of each one of the extruded layers. Three different values were considered: 0.18, 0.25, and 0.33 mm. The GrabCAD does not allow to select

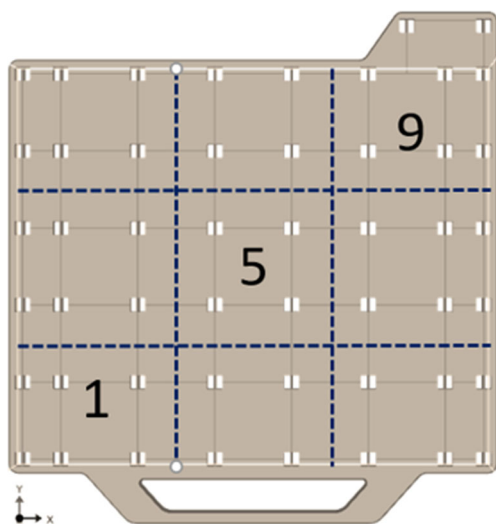


Fig. 6 Positions of the specimen on the build platform

distinct values from the previous ones because they are dependent on the F270 printer nozzle characteristics.

3.3.2 Infill pattern

Filling pattern is the variable that facilitates the user to pick a design to build the internal structure of the piece. Various possibilities can be selected depending on the software used to print the part. Among all options, infill patterns shown in Fig. 3 were preferred because they give adequate structural integrity.

3.3.3 Orientation angle

The orientation angle is the angle at which the part is oriented on the printing plane. Three distinct values were adopted for this research: 0, 45, and 90° (Fig. 4).

3.3.4 Printing plane

Printing planes XY, XZ, and YZ were used in the experimental trials. They are shown in Fig. 5.

3.3.5 Table position

This parameter is associated with part’s position on the build platform. The total area of the build platform was divided into

Table 1 Factors and their levels

Factor	Level 1	Level 2	Level 3
Layer thickness (mm)	0.18	0.25	0.33
Filling pattern	Solid	Sparse double dense	Hexagonal
Orientation angle (°)	0	45	90
Printing plane	XY	XZ	YZ
Table position	1	5	9

Table 2 Experimental results obtained in 3D printing of ASA

Run	Time (h)	Energy (kWh)	ΔW_{outer} (mm)	ΔW_{inner} (mm)	ΔL (mm)	ΔT (mm)	Model material (cm^3)	Support material (cm^3)	Yield strength (MPa)	UTS (MPa)
1	0.200	0.130	0.00	0.03	0.16	0.13	1.910	1.254	16.23	21.55
2	1.583	1.029	0.15	0.07	0.38	0.11	4.071	9.642	7.18	9.07
3	0.933	0.607	0.10	0.01	0.33	0.09	7.786	0.487	11.12	12.74
4	0.367	0.238	0.06	0.02	0.29	0.08	2.364	1.326	18.70	22.59
5	1.750	1.138	0.05	0.07	0.12	0.05	4.071	9.665	4.84	10.17
6	0.200	0.130	0.04	0.06	0.11	0.18	1.864	1.254	26.44	30.54
7	0.383	0.249	0.11	0.23	0.08	0.01	2.362	1.324	22.38	26.12
8	0.183	0.119	0.06	0.13	0.17	0.24	1.734	1.237	14.68	32.20
9	1.167	0.758	0.17	0.02	0.25	0.07	7.854	0.489	3.57	4.39
10	0.133	0.087	0.07	0.09	0.02	0.29	2.288	1.386	18.96	25.05
11	1.133	0.737	0.23	0.09	0.08	0.02	5.501	9.306	4.55	6.19
12	0.633	0.412	0.02	0.02	0.00	0.02	10.320	0.563	3.42	8.53
13	0.233	0.152	0.00	0.00	0.12	0.03	2.864	1.556	11.07	13.93
14	1.217	0.791	0.09	0.05	0.63	0.05	5.504	9.320	0.42	2.36
15	0.117	0.076	0.04	0.06	0.04	0.29	2.074	1.384	15.36	23.77
16	0.233	0.152	0.29	0.25	0.13	0.08	2.862	1.527	15.25	26.24
17	0.117	0.076	0.01	0.06	0.20	0.27	2.049	1.367	20.58	26.04
18	0.683	0.444	0.11	0.08	0.12	0.09	10.179	0.563	3.31	4.64
19	0.100	0.065	0.10	0.06	0.22	0.22	2.436	1.598	18.68	25.20
20	1.583	1.029	0.08	0.00	0.14	0.10	4.071	9.642	7.61	9.29
21	0.400	0.260	0.12	0.07	0.29	0.05	11.179	0.607	4.07	12.92
22	0.167	0.108	0.07	0.02	0.35	0.04	3.036	1.705	8.50	14.51
23	1.067	0.693	0.01	0.14	0.20	0.10	5.649	10.043	3.34	8.41
24	0.100	0.065	0.04	0.02	0.19	0.05	2.323	1.598	20.01	28.21
25	0.167	0.108	0.10	0.12	0.12	0.06	3.033	1.692	18.25	24.44
26	0.083	0.054	0.06	0.03	0.41	0.23	2.278	1.577	21.01	24.36
27	0.567	0.368	0.10	0.12	0.71	0.08	11.121	0.606	3.44	4.21

nine regions (Fig. 6). Positions 1, 5, and 9 correspond to the experimental runs.

3.4 Design of the experiment

The Taguchi method was developed by Genichi Taguchi to improve the quality control of products or processes. This method provides orthogonal arrays to execute experimental trials, a signal to noise (S/N) ratio graph to reduce process variability, and a means graph to adjust the process to the desired value.

An L27 array was adopted to analyze the impact of process parameters on the variables. For each one of the 27 trials included in the design, three repetitions were performed in a randomized order. In total, the F270 printer fabricated 81 specimens.

Restrictions imposed by the GrabCAD software and the ones of the 3D printer were considered along to the material

to be used (ASA) to select the levels of the L27 array. Table 1 presents the process parameters and their levels.

According to the Taguchi method, process variability decreases when the S/N ratio is at its maximum value. There are three categories for S/N ratio: nominal is the best, larger the better, and smaller the better. Depending on the purpose of the research, the experimenter should decide which one is the most appropriate. Processing time, energy consumption, dimensional deviation, and quantity of material were analyzed using the S/N ratio smaller the better. For yield strength and ultimate tensile strength, the S/N ratio larger is better was preferred because these variables should be maximized for enhancing the structural performance of the part.

The S/N ratio “smaller the better” was computed according to Eq. 2, and the one corresponding to the “larger the better” characteristic was obtained using Eq. 3.

$$S/N = -10 \log \left[(1/n) (\sum y^2) \right] \quad (2)$$

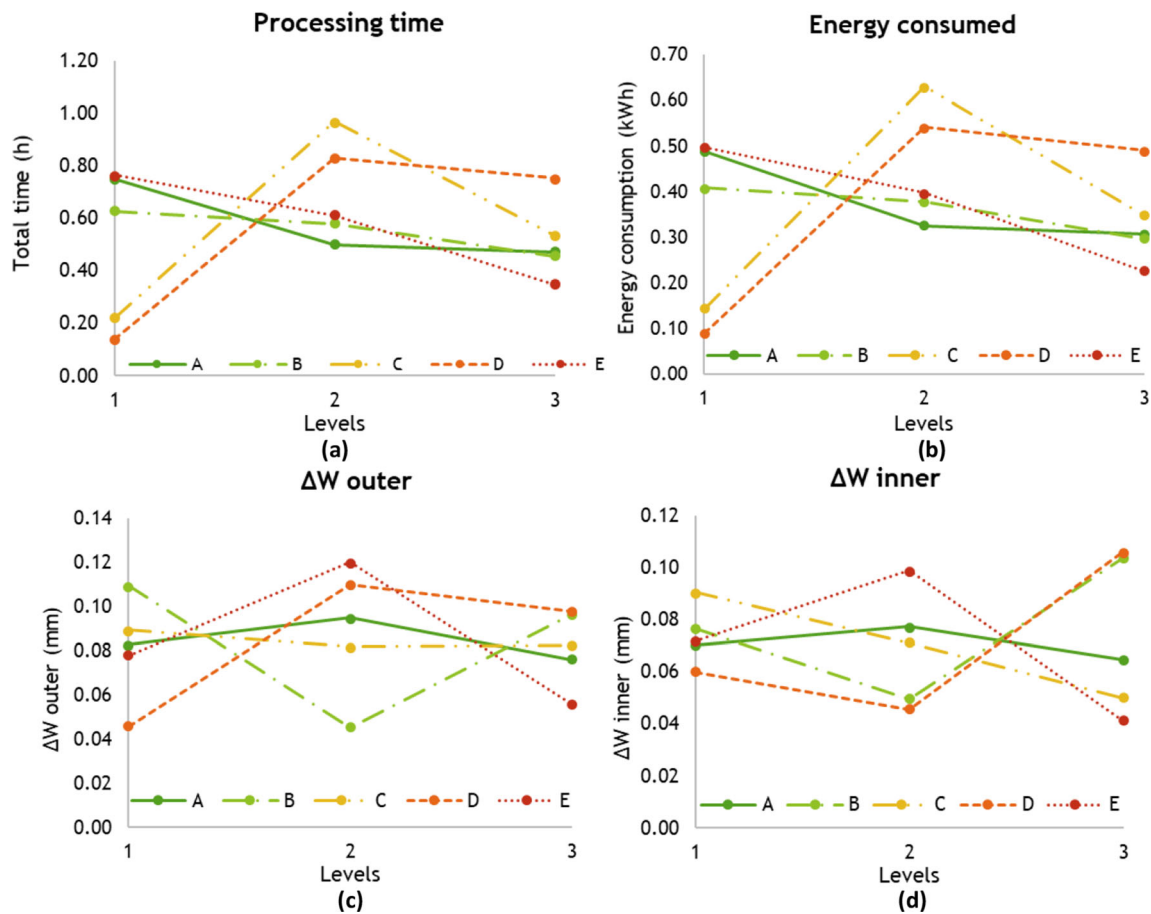


Fig. 7 Mean effects plot. a Processing time. b Energy consumed. c ΔW_{outer}. d ΔW_{inner}

$$S/N = -10\log\left[\frac{\sum(1/y^2)}{n}\right] \tag{3}$$

4 Results and data analysis

Table 2 presents the results acquired for processing time, energy drawn from the grid by the 3D printer, dimensional accuracy for the dimensions illustrated in Fig. 1 (ΔW_{outer}, ΔW_{inner}, ΔL, and ΔT), the quantity of model and support material, yield strength, and ultimate tensile strength (UTS). Figures 7, 8, and 9 correspond to the means analysis, and Figs. 10, 11, and 12 are the ones for the S/N ratio graphs for each one of the variables.

As stated by the main effects plot for processing time (Fig. 7a), the lowest value of this variable is reached when the layer thickness is at its maximum level with a hexagram filling pattern, the specimen oriented at 0° in the XY plane, using position 9 of the build platform. Peng et al. [15] inferred that the highest value of layer thickness provided the lowest printing time. Tanoto et al. [23] and Raut et al. [17] found that the time demanded to build the part is decreased when printed at 0° in the XY plane.

When layer thickness increases, the number of layers needed to build the part is reduced, thus minimizing processing time. The hexagram pattern, when compared with the solid and the sparse double dense ones, contains a smaller amount of material due to its structure. A reduction in printing time is achieved with a smaller quantity of extruded material. Moreover, the upper right corner of the build platform is the position at which the machine cleans the nozzle after building each layer. The outlet is moved to that point once it completes the layer. Position 9 of the platform is the nearest to the purge point, and this helps in decreasing the processing time. Moreover, if the position of the piece is at 90° in the XZ and YZ planes, printing time increases due to the higher number of layers required to build the part in that direction. Chaudhari et al. [6] presented the same conclusion.

The energy expended exhibited a similar trend as the one of printing time (Fig. 7b). The levels that decreased processing time are the ones that minimized energy consumption. The printer demands a certain amount of energy to run a process, and if that process lasts for a long time, the quantity of energy needed increases. Al-Ghamdi [4] also found out that an increment in the layer thickness lessens the overall energy consumption.

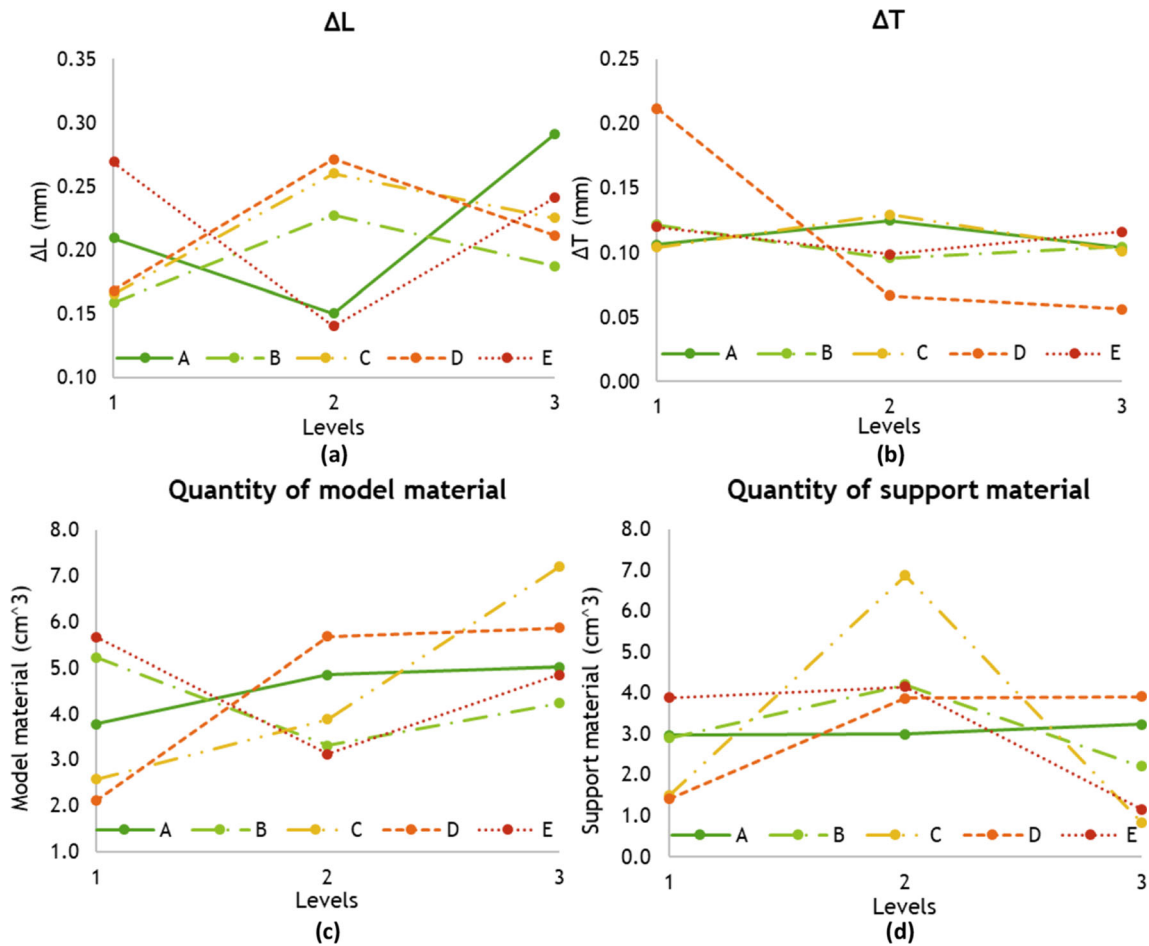


Fig. 8 Mean effects plot. a ΔL . b ΔT . c Quantity of model material. d Quantity of support material

The dimensional deviation corresponding to W_{outer} diminished when layer thickness increased its value applying the sparse double as the filling pattern, with the part oriented at 45° in the XY plane and printing it in position 9 of the platform (Fig. 7c). Tanoto et al. [23] and Alafaghani et al. [2] inferred that parts printed in the XY plane showed the least

dimensional variation. Moreover, Padhi et al. [14] and Peng et al. [15] manifested that dimensional difference decreases when the value of layer thickness rises.

The value of the ΔW_{inner} displayed in Fig. 7d was lowered when layer thickness was risen using a solid filling pattern, with an orientation angle of 90° in the XZ plane, and applying

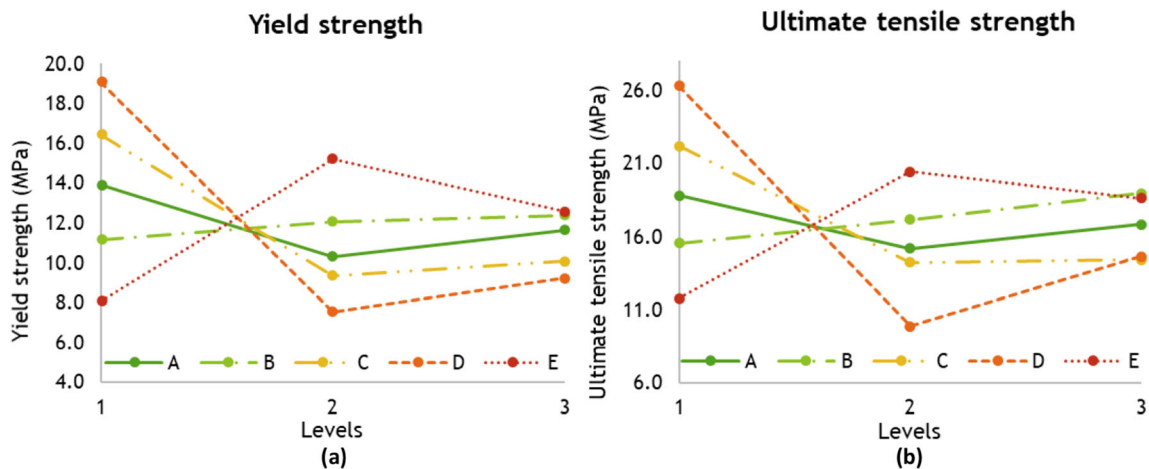


Fig. 9 Mean effects plot. a Yield strength. b Ultimate tensile strength

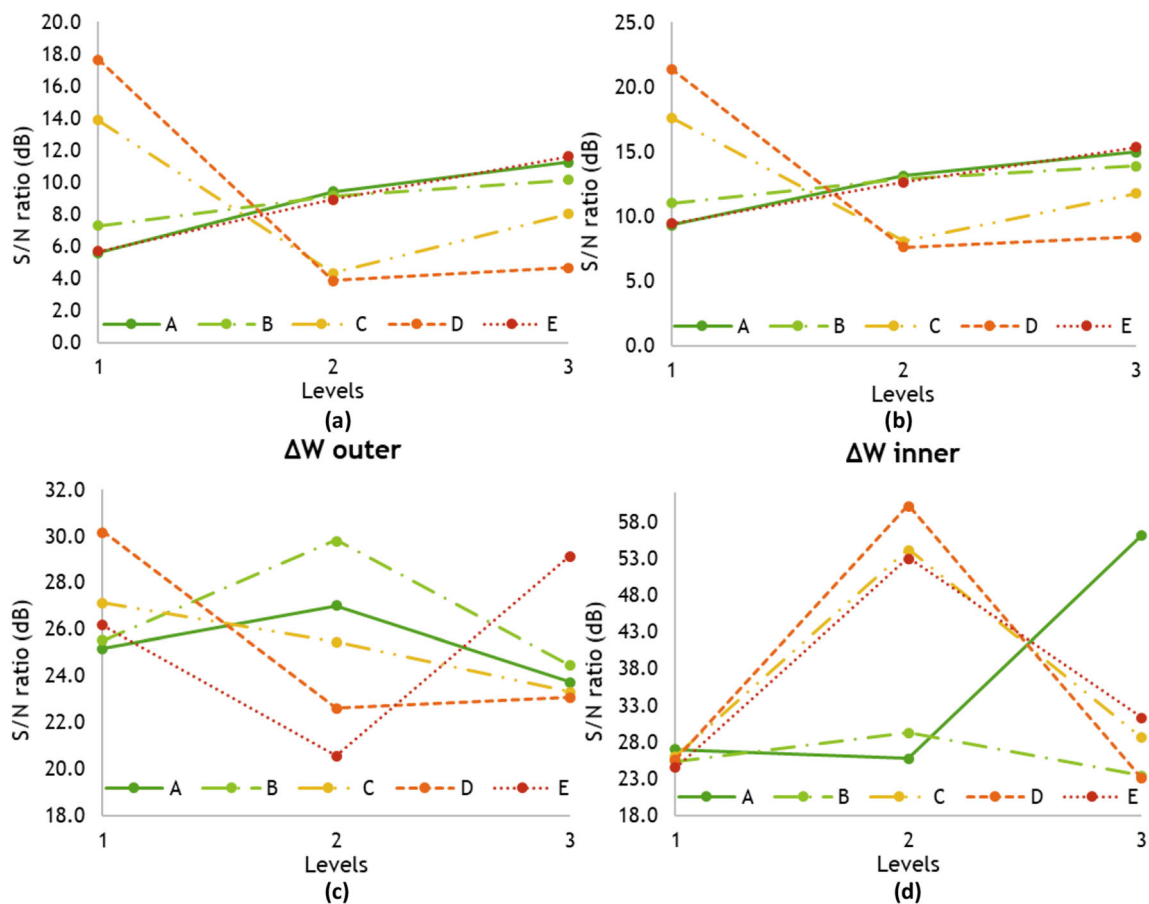


Fig. 10 S/N ratio plot. **a** Processing time. **b** Energy consumed. **c** ΔW_{outer} . **d** ΔW_{inner}

position 9 of the build platform. Alafaghani et al. [2] concluded out that the XZ plane gave the lowest dimensional variation about ΔW_{inner} , and Singh et al. [19] concluded that solid filling pattern was the one that reached the greatest dimensional exactness.

As stated in the main effects plot for dimensional accuracy regarding L (Fig. 8a), the second level of thickness layer and solid filling pattern, along with an orientation angle of 0° in the XY plane, and position 5 of the build platform, reduced the dimensional deviation of the specimen's length. Huynh et al. [11] and Padhi et al. [14] found out the same results for layer thickness and Alafaghani et al. [2] for the building plane.

The thickness dimensional variation (ΔT , Fig. 8b) was lowered at the largest value of layer thickness, with the sparse double dense pattern and a part orientation at 90° in the YZ plane, using position 5 of the platform. Peng et al. [15] deduced that the highest layer height minimized thickness' dimensional deviation. According to Alafaghani et al. [2], the Y plane, when used, allowed to enhance dimensional accuracy.

Regarding the quantity of model material (Fig. 8c), the smallest value of the layer thickness lowered it, along with a sparse double dense pattern, an orientation angle of 0° in the XY plane, employing position 5 of the build platform. Al-Ghamdi [4] explored the impact of layer thickness, among

other parameters, on specific consumed mass used to create a cube made of ABS. The results exhibited that a smaller layer thickness decreased the specific mass of the model.

For the case of the quantity of support material, the configuration that obtained the lowest value is the one corresponding to the smallest layer thickness with a hexagonal infill pattern, using an orientation angle of 90° in the XY plane and position 5 of the build platform (Fig. 8d). When the piece is oriented at 45° in the XZ plane (worst set of process parameters), the support material surrounds the part, thus increasing its quantity.

Concerning the yield strength of the part, the layer thickness at its minimum level with a hexagram filling pattern, the specimen oriented at 0° in the XY plane, using position 5 of the build platform, improved it (Fig. 9a). Even though the feedstock used for FDM owns a set of mechanical properties, these are not the same as the ones exhibited by the printed specimen. One of the reasons is FDM uses layers that are joined together by locally melting the material of a previous extruded layer, which differs from other manufacturing operations, like the injection molding process [22].

Stratasys reported that the yield strength of the material, when printed in the XZ plane (according to ASTM D638 standard, using type 1 specimen), is equal to 27 MPa [20].

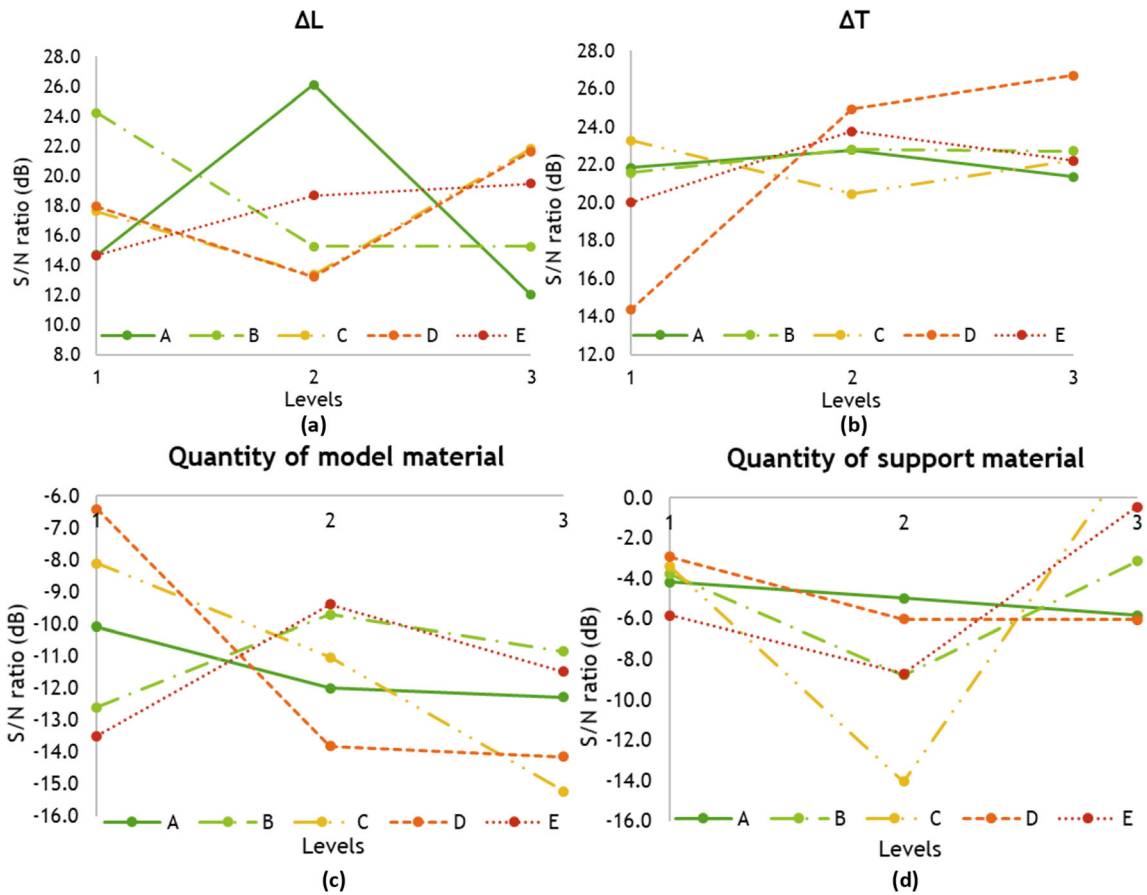


Fig. 11 S/N ratio plot. a ΔL . b ΔT . c Quantity of model material. d Quantity of support material

Test 7 corresponds to this printing plane, and the result was 22.38 MPa, 17% lower than the one stated by Stratasys. Alaimo et al. [3] concluded that mechanical properties of parts rely on fiber orientation; specimens oriented at 0° exhibited a ductile behavior, and the ones oriented at 90° showed a brittle performance. Fayazbakhsh et al. [8] stated the same conclusion. Chacón et al. [5] found out that a reduction in layer thickness increased specimen stiffness.

Finally, the values of the process parameters that increased ultimate tensile strength are the same as the ones that enhanced yield strength (Fig. 9b). Samykano et al. [18] and Kerekes et al. [25] concluded that the higher the infill percentage, the higher the value of UTS, and this is coincident to the results found in the experimental trials. Stratasys stated that yield strength of the material, when printed in the XZ plane (according to ASTM D638 standard, using type 1 specimen),

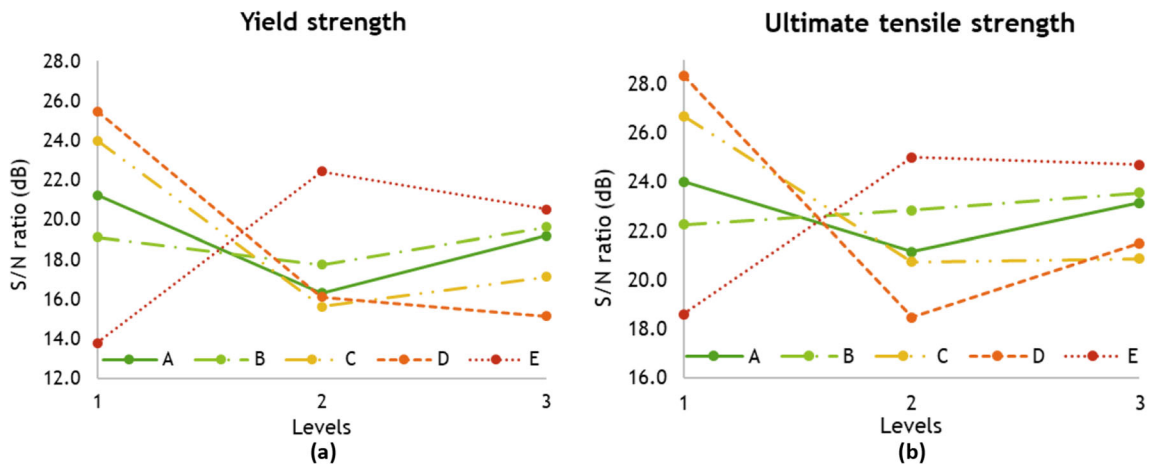


Fig. 12 S/N ratio plot. a Yield strength. b Ultimate tensile strength

Table 3 ANOVA for means—processing time

Factor	DoF	SS	Adj SS	Adj MS	<i>F</i>	<i>P</i>	% contribution
Layer thickness	2	0.431	0.43062	0.21531	7.32	0.046	5.90
Filling pattern	2	0.540	0.54006	0.27003	9.18	0.032	7.40
Orientation angle	2	2.54117	2.54117	1.27059	43.2	0.002	34.84
Printing plane	2	2.60574	2.60574	1.30287	44.29	0.002	35.73
Table position	2	0.80673	0.80673	0.40336	13.71	0.016	11.06
Layer thickness*filling pattern	2	0.0208	0.0208	0.0052	0.18	0.939	0.29
Layer thickness*orientation angle	2	0.08173	0.08173	0.02043	0.69	0.634	1.12
Layer thickness*printing plane	2	0.14901	0.14901	0.03725	1.27	0.412	2.04
Residual error	4	0.11765	0.11765	0.02941			
Total	26	7.29352					

$S = 0.1715$, $R\text{-Sq} = 98.39\%$, $R\text{-Sq}(\text{adj}) = 89.51\%$

is equal to 30 MPa [20]. The result of test 7 was 26.12 MPa, 13% lower than the one provided by Stratasys.

S/N ratio plots for all the variables are shown in Figs. 10, 11, and 12. The levels of process parameters that optimized the variables are equal to the values that lowered process variation; this applies to the processing time, energy consumed, dimensional accuracy of the specimen’s length, the quantity of both model and support material, yield strength, and ultimate tensile strength. Dimensional accuracy of the specimen’s outer and inner width and the one related to the specimen’s thickness were the variables that did not show the same trend.

An analysis of variance (ANOVA) and an *F* test were performed to explain the significance of each factor. These analyses considered a confidence level of 95%. The printing plane was the most significant factor for minimizing processing time and energy. Dimensional precision for width (outer and inner) is affected the most by filling pattern. Dimensional variation of the specimen’s length and thickness is influenced by layer thickness and printing plane, respectively. Quantity of model

and support material is affected by the orientation angle, and the mechanical properties of the specimen (yield strength and ultimate tensile strength) are determined by the printing plane.

The analysis of variance (ANOVA) performed for each one of the response variables is shown in Tables 3, 4, 5, 6, 7, 8, 9, 10, 11, and 12, as well as the percentage of contribution of the studied factors.

4.1 Desirability and comparative analyses

As stated by the previous results, the values of process parameters that strengthen one of the variables were not the same for the other responses. As a consequence, to optimize all the variables at the same time, a desirability analysis was conducted. The software used to execute the analysis was Minitab v18, and the values of weight and importance for each one of the variables were established. For this study, both values were set to one, which means all the variables are equally relevant for the optimization process. The desirability analysis

Table 4 ANOVA for means—energy consumed

Factor	DoF	SS	Adj SS	Adj MS	<i>F</i>	<i>P</i>	% contribution
Layer thickness	2	0.18194	0.18194	0.090968	7.32	0.046	5.90
Filling pattern	2	0.22818	0.22818	0.114088	9.18	0.032	7.40
Orientation angle	2	1.07365	1.07365	0.536823	43.2	0.002	34.84
Printing plane	2	1.10093	1.10093	0.550463	44.29	0.002	35.73
Table position	2	0.34084	0.34084	0.170421	13.71	0.016	11.06
Layer thickness*filling pattern	2	0.00879	0.00879	0.002197	0.18	0.939	0.29
Layer thickness*orientation angle	2	0.03453	0.03453	0.008633	0.69	0.634	1.12
Layer thickness*printing plane	2	0.06296	0.06296	0.015739	1.27	0.412	2.04
Residual error	4	0.04971	0.04971	0.012427			
Total	26	3.08151					

$S = 0.1115$, $R\text{-Sq} = 98.39\%$, $R\text{-Sq}(\text{adj}) = 89.51\%$

Table 5 ANOVA for means— ΔW_{outer}

Factor	DoF	SS	Adj SS	Adj MS	F	P	% contribution
Layer thickness	2	0.001643	0.001643	0.000822	1.32	0.362	1.43
Filling pattern	2	0.021476	0.021476	0.010738	17.32	0.011	18.65
Orientation angle	2	0.000304	0.000304	0.000152	0.25	0.793	0.26
Printing plane	2	0.021089	0.021089	0.010544	17	0.011	18.31
Table position	2	0.019289	0.019289	0.009644	15.55	0.013	16.75
Layer thickness*orientation angle	2	0.012624	0.012624	0.003156	5.09	0.072	10.96
Layer thickness*printing plane	2	0.008726	0.008726	0.002182	3.52	0.125	7.58
Layer thickness*table position	2	0.027522	0.027522	0.006881	11.1	0.019	23.90
Residual error	4	0.002481	0.002481	0.00062			
Total	26	0.115154					

$S = 0.0249$, R-Sq = 97.85%, R-Sq (adj) = 86.00%

returns values in the range from zero to one, being one the most suitable. Table 13 displays the results of this analysis.

From Table 13, solution 1 is the one that obtained a desirability value nearby to one. Therefore, this set of process parameters was the one that optimized all the variables at the same time. An experimental test was conducted for validating these results executing three repetitions, and the values gathered are shown in Table 14, as well as the difference (expressed as a percentage) between the predicted value and the average result of the three experimental trials. According to the information presented in Table 14, the difference between the experimental results and the predicted ones was lower than 10%.

It is relevant to notice that this combination of values increased specific responses and worsened the others. Table 15 shows a comparison between the desirability analysis

experimental results, and the experimental results obtained when one variable was optimized at a time using the Taguchi methodology. Scenario 1 corresponds to the desirability analysis, and the minimum processing time, energy consumed, ΔW_{outer} , ΔW_{inner} , ΔL , ΔT , the quantity of model material, and quantity of support material correspond to scenarios 2, 3, 4, 5, 6, 7, 8, and 9, respectively. The maximum yield strength is related to scenario 10, and scenario 11 to the maximum ultimate tensile strength.

The desirability analysis provided a greater dimensional accuracy for the width (inner) and the thickness of the specimen when compared with the results obtained by the Taguchi method. These variables were reduced by 76 and 30%, respectively. For the other variables, this analysis presented a variables' increment that went from 11 (ΔL) to 85% (ΔW_{outer}). Although the desirability analysis did not provide the best

Table 6 ANOVA for means— ΔW_{inner}

Factor	DoF	SS	Adj SS	Adj MS	F	P	% contribution
Layer thickness	2	0.000739	0.000739	0.000369	0.61	0.585	0.74
Filling pattern	2	0.026017	0.026017	0.013008	21.63	0.007	26.14
Orientation angle	2	0.007406	0.007406	0.003703	6.16	0.06	7.44
Printing plane	2	0.018006	0.018006	0.009003	14.97	0.014	18.09
Table position	2	0.015039	0.015039	0.007519	12.5	0.019	15.11
Layer thickness*filling pattern	2	0.003711	0.003711	0.000928	1.54	0.342	3.73
Layer thickness*orientation angle	2	0.007339	0.007339	0.001835	3.05	0.153	7.37
Layer thickness*table position	2	0.018856	0.018856	0.004714	7.84	0.036	18.95
Residual error	4	0.002406	0.002406	0.000601			
Total	26	0.099517					

$S = 0.0245$, R-Sq = 97.58%, R-Sq (adj) = 84.29%

Table 7 ANOVA for means— ΔL

Factor	DoF	SS	Adj SS	Adj MS	F	P	% contribution
Layer thickness	2	0.0664	0.16391	0.081957	10.69	0.043	9.50
Filling pattern	2	0.01004	0.07805	0.039024	5.09	0.109	1.44
Orientation angle	2	0.04551	0.06052	0.030262	3.95	0.145	6.51
Printing plane	2	0.0487	0.08146	0.040729	5.31	0.103	6.97
Table position	2	0.09593	0.084	0.042	5.48	0.1	13.72
Layer thickness*filling pattern	2	0.13062	0.2341	0.058525	7.63	0.063	18.69
Layer thickness*orientation angle	2	0.12472	0.20959	0.052397	6.83	0.073	17.84
Layer thickness*table position	2	0.15408	0.15408	0.038519	5.02	0.108	22.04
Residual error	4	0.023	0.023	0.007668			
Total	26	0.699					

$S = 0.0876$, $R\text{-Sq} = 96.71\%$, $R\text{-Sq (adj)} = 72.58\%$

value for all the variables, it achieved a good trade-off among them.

5 Conclusions

An experimental study was conducted to optimize several variables associated with the part quality, productivity, and sustainability of FDM, using ASA as model material. These variables are part’s dimensional exactitude regarding its width, length, and thickness, the time needed to create the piece, and the material used for building it (model and support material). Finally, the energy consumed during 3D printing was acknowledged as a means of process sustainability.

Five parameters were modified to study the influence of process parameters on variables’ behavior, using an orthogonal array: layer thickness, filling pattern, orientation angle, printing plane, and position of the part on the build platform.

Taguchi methodology and an ANOVA assisted in examining the parameters and their impact on the variables, and the results denoted the printing plane was the factor with the largest effect on processing time, energy spent, dimensional precision of part thickness, yield strength, and ultimate tensile strength.

For the specimen’s width dimensional accuracy (outer and inner), the filling pattern influenced this variable. Finally, part’s orientation angle was the parameter with the principal influence over the quantity of both model and support materials. Furthermore, to determine a set of parameters that allowed a simultaneous optimization of all the variables, a desirability analysis was executed.

According to the results, 0.33 mm of layer thickness, using the sparse double dense filling pattern with an orientation angle of 90° in the XY plane, and position number 5 of the build platform, obtained the most suitable value of desirability. Considering the results gathered with this set of parameters, and the ones provided by the Taguchi methodology, the

Table 8 ANOVA for means— ΔT

Factor	DoF	SS	Adj SS	Adj MS	F	P	% contribution
Layer thickness	2	0.002475	0.002475	0.001237	0.89	0.48	1.23
Filling pattern	2	0.003927	0.003927	0.001963	1.41	0.345	1.95
Orientation angle	2	0.004366	0.004366	0.002183	1.56	0.315	2.16
Printing plane	2	0.136301	0.136301	0.068151	48.79	0.002	67.53
Table position	2	0.002287	0.002287	0.001144	0.82	0.503	1.13
Layer thickness*orientation angle	2	0.012642	0.012642	0.003161	2.26	0.224	6.26
Layer thickness*printing plane	2	0.024157	0.024157	0.006039	4.32	0.093	11.97
Layer thickness*table position	2	0.010108	0.010108	0.002527	1.81	0.29	5.01
Residual error	4	0.005587	0.005587	0.001397			
Total	26	0.20185					

$S = 0.0374$, $R\text{-Sq} = 97.23\%$, $R\text{-Sq (adj)} = 82.01\%$

Table 9 ANOVA for means—model material

Factor	DoF	SS	Adj SS	Adj MS	<i>F</i>	<i>P</i>	% contribution
Layer thickness	2	8.084	8.084	4.0422	25.84	0.005	3.22
Filling pattern	2	22.888	22.888	11.4438	73.16	0.001	9.11
Orientation angle	2	101.888	101.888	50.9438	325.66	0	40.55
Printing plane	2	80.621	80.621	40.3103	257.69	0	32.09
Table position	2	30.208	30.208	15.1042	96.56	0	12.02
Layer thickness*orientation angle	2	3.241	3.241	0.8102	5.18	0.07	1.29
Layer thickness*printing plane	2	1.964	1.964	0.4909	3.14	0.147	0.78
Layer thickness*table position	2	1.738	1.738	0.4345	2.78	0.173	0.69
Residual error	4	0.626	0.626	0.1564			
Total	26	251.257					

$S = 0.3955$, $R\text{-Sq} = 99.75\%$, $R\text{-Sq}(\text{adj}) = 98.38\%$

desirability analysis allowed finding a good trade-off among the responses of 3D printing. As a consequence, it improved the sustainability of the process without a significant reduction in productivity and part quality.

Acknowledgments The author would like to thank Tecnológico de Monterrey Campus Toluca for providing a 3D printer and material for conducting the experimental trials.

Data availability The raw/processed data required to reproduce these findings cannot be shared at this time as data also form part of an ongoing study.

References

- 52900:2015, A (2015) Standard terminology for additive manufacturing—general principles—terminology. ASTM Int. <https://doi.org/10.1520/F2792-12A.2>
- Alafaghani A, Qattawi A, Alrawi B, Guzman A (2017) Experimental optimization of fused deposition modelling processing parameters: a design-for-manufacturing approach. *Procedia Manuf* 10:791–803. <https://doi.org/10.1016/j.promfg.2017.07.079>
- Alaimo G, Marconi S, Costato L, Auricchio F (2017) Influence of meso-structure and chemical composition on FDM 3D-printed parts. *Compos B Eng* 113:371–380. <https://doi.org/10.1016/J.COMPOSITESB.2017.01.019>
- Al-Ghamdi KA (2019) Sustainable FDM additive manufacturing of ABS components with emphasis on energy minimized and time efficient lightweight construction. *Int J Light Mater Manuf* 2:338–345. <https://doi.org/10.1016/j.ijlmm.2019.05.004>
- Chacón JM, Caminero MA, García-Plaza E, Núñez PJ (2017) Additive manufacturing of PLA structures using fused deposition modelling: effect of process parameters on mechanical properties and their optimal selection. *Mater Des* 124:143–157. <https://doi.org/10.1016/j.matdes.2017.03.065>
- Chaudhari M, Jogi BF, Pawade RS (2018) Comparative study of part characteristics built using additive manufacturing (FDM). *Procedia Manuf*. <https://doi.org/10.1016/j.promfg.2018.02.010>
- Conway KM, Pataky GJ (2019) Cracking in additively manufactured acrylonitrile butadiene styrene. *Eng Fract Mech* 211:114–124. <https://doi.org/10.1016/J.ENGFRACMECH.2019.02.020>
- Fayazbakhsh K, Movahedi M, Kalman J (2019) The impact of defects on tensile properties of 3D printed parts manufactured by fused filament fabrication. *Mater Today Commun* 18:140–148. <https://doi.org/10.1016/j.mtcomm.2018.12.003>

Table 10 ANOVA for means—support material

Factor	DoF	SS	Adj SS	Adj MS	<i>F</i>	<i>P</i>	% contribution
Layer thickness	2	0.377	0.377	0.1887	19.03	0.009	0.11
Filling pattern	2	49.883	49.883	24.9413	2514.53	0	14.93
Orientation angle	2	197.12	197.12	98.5601	9936.62	0	59.00
Printing plane	2	37.098	37.098	18.549	1870.07	0	11.10
Table position	2	49.339	49.339	24.6696	2487.14	0	14.77
Layer thickness*filling pattern	2	0.066	0.066	0.0166	1.67	0.315	0.02
Layer thickness*orientation angle	2	0.147	0.147	0.0368	3.71	0.116	0.04
Layer thickness*printing plane	2	0.041	0.041	0.0102	1.03	0.49	0.01
Residual error	4	0.04	0.04	0.0099			
Total	26	334.112					

$S = 0.0996$, $R\text{-Sq} = 99.99\%$, $R\text{-Sq}(\text{adj}) = 99.92\%$

Table 11 ANOVA for means—yield strength

Factor	DoF	SS	Adj SS	Adj MS	F	P	% contribution
Layer thickness	2	58.95	58.95	29.476	3.08	0.155	3.96
Filling pattern	2	52.34	52.34	26.17	2.74	0.178	3.52
Orientation angle	2	273.94	273.94	136.971	14.33	0.015	18.41
Printing plane	2	701.54	701.54	350.77	36.7	0.003	47.16
Table position	2	234.37	234.37	117.184	12.26	0.02	15.75
Layer thickness*filling pattern	2	51.58	51.58	12.896	1.35	0.389	3.47
Layer thickness*orientation angle	2	44.77	44.77	11.193	1.17	0.441	3.01
Layer thickness*printing plane	2	31.9	31.9	7.975	0.83	0.568	2.14
Residual error	4	38.23	38.23	9.557			
Total	26	1487.63					

S = 3.0915, R-Sq = 97.43%, R-Sq (adj) = 83.30%

9. Guessasma S, Belhabib S, Nouri H (2019) Microstructure, thermal and mechanical behavior of 3D printed acrylonitrile styrene acrylate. *Macromol Mater Eng* 304:1800793. <https://doi.org/10.1002/mame.201800793>

10. Hassanifard S, Hashemi SM (2020) On the strain-life fatigue parameters of additive manufactured plastic materials through fused filament fabrication process. *Addit Manuf* 32:100973. <https://doi.org/10.1016/j.addma.2019.100973>

11. Huynh HN, Nguyen AT, Ha NL, Ha Thai TT (2017) Application of fuzzy Taguchi method to improve the dimensional accuracy of fused deposition modeling processed product. In: *Proceedings - 2017 International Conference on System Science and Engineering, ICSSE 2017*. <https://doi.org/10.1109/ICSSE.2017.8030847>

12. Mohamed OA, Masood SH, Bhowmik JL (2016) Optimization of fused deposition modeling process parameters for dimensional accuracy using I-optimality criterion. *Meas J Int Meas Confed* 81: 174–196. <https://doi.org/10.1016/j.measurement.2015.12.011>

13. Murr LE (2021) Rapid prototyping technologies: solid freedom fabrication, in: *Handbook of materials structures, properties, processing and performance*. Springer International Publishing, Cham, pp 1–13. https://doi.org/10.1007/978-3-319-01905-5_37-1

14. Padhi SK, Sahu RK, Mahapatra SS, Das HC, Sood AK, Patro B, Mondal AK (2017) Optimization of fused deposition modeling process parameters using a fuzzy inference system coupled with Taguchi philosophy. *Adv Manuf* 5:231–242. <https://doi.org/10.1007/s40436-017-0187-4>

15. Peng A, Xiao X, Yue R (2014) Process parameter optimization for fused deposition modeling using response surface methodology combined with fuzzy inference system. *Int J Adv Manuf Technol* 73:87–100. <https://doi.org/10.1007/s00170-014-5796-5>

16. Rashid A (2018) Additive manufacturing technologies. In: Chatti S, Tolio T (eds) *CIRP encyclopedia of production engineering*. Springer, Berlin, pp 1–9. https://doi.org/10.1007/978-3-642-35950-7_16866-1

17. Raut S, Jatti VS, Khedkar NK, Singh TP (2014) Investigation of the effect of built orientation on mechanical properties and total cost of FDM parts. *Procedia Mater Sci* 6:1625–1630. <https://doi.org/10.1016/j.mspro.2014.07.146>

18. Samykano M, Selvamani SK, Kadirgama K, Ngui WK, Kanagaraj G, Sudhakar K (2019) Mechanical property of FDM printed ABS: influence of printing parameters. *Int J Adv Manuf Technol* 102: 2779–2796. <https://doi.org/10.1007/s00170-019-03313-0>

19. Singh R, Singh S, Singh IP, Fabbrocino F, Fraternali F (2017) Investigation for surface finish improvement of FDM parts by

Table 12 ANOVA for means—ultimate tensile strength

Factor	DoF	SS	Adj SS	Adj MS	F	P	% contribution
Layer thickness	2	59.26	59.26	29.631	3.84	0.117	2.57
Filling pattern	2	99.09	99.09	49.545	6.42	0.056	4.31
Orientation angle	2	369.54	369.54	184.768	23.93	0.006	16.06
Printing plane	2	1289.87	1289.87	644.936	83.53	0.001	56.04
Table position	2	375.91	375.91	187.956	24.34	0.006	16.33
Layer thickness*filling pattern	2	56.39	56.39	14.098	1.83	0.287	2.45
Layer thickness*orientation angle	2	16.56	16.56	4.139	0.54	0.72	0.72
Layer thickness*printing plane	2	4	4	0.999	0.13	0.964	0.17
Residual error	4	30.89	30.89	7.721			
Total	26	2301.5					

S = 2.7787, R-Sq = 98.66%, R-Sq (adj) = 91.28%

Table 13 Solutions from the desirability analysis

Solution	Layer thickness (mm)	Filling pattern	Orientation angle (°)	Printing plane	Table position	Desirability value
1	0.33	Sparse double dense	90	XY	5	0.8655
2	0.33	Sparse double dense	90	XY	1	0.7045
3	0.25	Solid	0	XY	1	0.7135
4	0.33	Hexagram	87	XY	5	0.7803
5	0.18	Sparse double dense	90	XY	5	0.7587

- vapor smoothing process. *Compos B Eng* 111:228–234. <https://doi.org/10.1016/j.compositesb.2016.11.062>
20. Stratasys Ltd. (2019) ASA Data Sheet [WWW Document]. URL <https://www.stratasys.com/materials/search/asa> (accessed 10.31.19)
 21. Sutherland JW, Gunter KL (2001) Environmental attributes of manufacturing processes. In: Handbook of environmentally conscious manufacturing. https://doi.org/10.1007/978-1-4615-1727-6_13
 22. Tabacu S, Ducu C (2018) Experimental testing and numerical analysis of FDM multi-cell inserts and hybrid structures. *Thin-Walled Struct* 129:197–212. <https://doi.org/10.1016/j.tws.2018.04.009>
 23. Tanoto YY, Anggono J, Siahaan IH, Budiman W (2017) The effect of orientation difference in fused deposition modeling of ABS polymer on the processing time, dimension accuracy, and strength. in: AIP Conference Proceedings. <https://doi.org/10.1063/1.4968304>
 24. Verbeeten WMH, Lorenzo-Bañuelos M, Arribas-Subiñas PJ (2020) Anisotropic rate-dependent mechanical behavior of poly(lactic acid) processed by material extrusion additive manufacturing. *Addit Manuf* 31:100968. <https://doi.org/10.1016/j.addma.2019.100968>
 25. Webbe Kerekes T, Lim H, Joe WY, Yun GJ (2019) Characterization of process–deformation/damage property relationship of fused deposition modeling (FDM) 3D-printed specimens. *Addit Manuf* 25: 532–544. <https://doi.org/10.1016/j.addma.2018.11.008>
 26. Zhao Y, Chen Y, Zhou Y (2019) Novel mechanical models of tensile strength and elastic property of FDM AM PLA materials: experimental and theoretical analyses. *Mater Des* 181:108089. <https://doi.org/10.1016/j.matdes.2019.108089>

Publisher's note Springer Nature remains neutral with regard to jurisdictional claims in published maps and institutional affiliations.

Table 14 Results achieved using the solution 1 of the desirability analysis

Variable	Model prediction	Experimental result	% difference
Total time (h)	0.123	0.120	2.52
Energy consumed (kWh)	0.080	0.078	2.50
ΔW_{outer} (mm)	0.034	0.037	– 8.96
ΔW_{inner} (mm)	0.017	0.016	2.69
ΔL (mm)	0.143	0.150	– 4.68
ΔT (mm)	0.063	0.064	– 1.52
Quantity of model material (cm ³)	2.449	2.408	1.67
Quantity of support material (cm ³)	1.6253	1.598	1.68
Yield strength (MPa)	20.812	19.677	5.45
Ultimate tensile strength (MPa)	28.163	28.612	– 1.60

Table 15 Comparison between the results achieved using the desirability analysis and the Taguchi methodology

Response	Scenarios											
	1	2	3	4	5	6	7	8	9	10	11	
Processing time (h)	0.120	0.10										
Energy consumed (kWh)	0.078		0.065									
ΔW_{outer} (mm)	0.037			0.02								
ΔW_{inner} (mm)	0.016				0.066							
ΔL (mm)	0.150					0.135						
ΔT (mm)	0.064						0.091					
Quantity of model material (cm ³)	2.408							1.911				
Quantity of support material (cm ³)	1.598								1.256			
Yield strength (MPa)	19.677									27.22		
Ultimate tensile strength (MPa)	28.612											34.18
Difference between scenarios (%)	-	20	20	85	- 76	11	- 30	26	27	- 28	- 16	